Infrared magnetic response in a random silicon carbide micropowder

Mark S. Wheeler,[1,*] J. Stewart Aitchison,[1] Jennifer I. L. Chen,[2] Geoffrey A. Ozin,[2] and Mohammad Mojahedi[1]
[1]*Department of Electrical and Computer Engineering, University of Toronto, Toronto, Ontario, Canada M5S 3G4*
[2]*Department of Chemistry, University of Toronto, Toronto, Ontario, Canada M5S 3H6*
(Received 13 August 2008; revised manuscript received 27 January 2009; published 23 February 2009)

We generalize the theoretical model of magnetic metamaterials made of dielectric particles to treat random particle sizes, shapes, and orientations. We demonstrate that the magnetic-dipole response of these randomly shaped subwavelength particles can be approximated with Mie theory as though they were spheres, while a quasistatic ellipsoidal approximation is used for the electric-dipole response. We verify our model with experimental measurement of a bulk magnetic response in a micropowder of milled SiC particles. Using such a crude powder could lead to immensely simplified negative permeability inclusions for negative index metamaterials.

DOI: 10.1103/PhysRevB.79.073103 PACS number(s): 78.20.Ci, 41.20.Jb, 77.84.Lf

There has been rapid progress recently in the fabrication of infrared and optical metamaterials. These are artificially structured composites with constituent elements much smaller than the wavelength of light. Metamaterials may possess electromagnetic properties not found in nature, such as a negative magnetic permeability or, by the simultaneous pairing of negative permeability and permittivity, a negative index of refraction. These metamaterials allow for applications such as superlensing[1] or invisibility cloaks.[2] Magnetic metamaterials are not only a crucial component in these applications, but are interesting in their own right. The most common approach to fabricating optical magnetic metamaterials is to make the constituent particles out of metallodielectric structures such as split-ring resonators (SRRs). More recently, variants such as staples, single rings, U shapes, and paired rods or strips have become preferred for optical metamaterials.[3] Fabrication of these structures is often limited to planar geometries, although recently four planes of SRRs were fabricated by a layer-by-layer technique.[4] Despite these impressive accomplishments, metamaterials composed of metallodielectric structures remain difficult to fabricate due to the intricate metallic patterns and tolerances and the need for sophisticated techniques and equipment. Furthermore, the metallic losses are large at optical frequencies. To avoid these problems, we and others have investigated the theoretical foundation for designing metamaterials using much simpler spherical inclusions. A negative permeability can be formed by a lattice of magnetodielectric or polaritonic spheres.[5–7] On the other hand, a negative index can be obtained by overlapping a negative permittivity using a second set of spheres[5,7] or a single set of coated spheres.[8] More recently, experimental verifications were reported, either of the magnetic-dipole scattering of single SiC whiskers[9] or of the negative permeability of a cubic lattice of ferroelectric cubes.[10]

In this Brief Report, we present a generalization of effective-medium theory for metamaterials made of large-permittivity dielectric particles to include particles with random sizes, shapes, and orientations. We also verify this experimentally with a sample of randomly shaped and oriented SiC microparticles. The sample was made by extremely simple mechanical techniques and is essentially nothing more than very fine sandpaper grit. Despite the randomness, the theory and experiment indicate a bulk magnetic response which is almost independent of particle shape and is hardly degraded from that predicted for an equivalent ordered lattice of spherical inclusions. Also, a bulk electric resonance is found which is considerably broadened by the wide variation of particle shapes. The results, particularly the magnetic response, suggest that such dielectric particles might be a much simpler alternative to SRRs for metamaterial fabrication.

We now summarize the effective-medium theory for dielectric-based magnetic metamaterials. A material composed of particles of various sizes, shapes, and orientations may be assigned an effective permittivity ε_{eff} and permeability μ_{eff} if the particles are much smaller than the wavelength in the host medium and if the density of particles is not "too great." In this case an incident field induces in general both electric- and magnetic-dipole responses in each particle. If a composite is made of N particles in a unit volume with permittivity $\varepsilon_s = n_s^2$ embedded in a host with permittivity $\varepsilon_h = n_h^2$, then the effective parameters are[8]

$$\frac{\mu_{\text{eff}} - \mu_0}{\mu_{\text{eff}} + 2\mu_0} = \frac{2\pi i N}{k_h^3}\overline{\langle b_1 \rangle}, \tag{1}$$

$$\frac{\varepsilon_{\text{eff}} - \varepsilon_h}{\varepsilon_{\text{eff}} + 2\varepsilon_h} = \frac{2\pi i N}{k_h^3}\overline{\langle a_1 \rangle}, \tag{2}$$

where k_h is the wave vector in the host and μ_0 is the permeability of the vacuum. The generalized electric- and magnetic-dipole scattering coefficients of any one particle are a_1 and b_1, respectively. The $\langle \cdot \rangle$ denotes size averaging and the overline indicates both shape and orientation averaging. If the particles are spheres with radius r_s, then our generalized dipole coefficients reduce to those of Mie theory, such that $a_1 = a_1^{\text{Mie}}$ and $b_1 = b_1^{\text{Mie}}$, where[11]

$$a_n^{\text{Mie}} = \frac{n_s \psi_n(n_s x)\psi_n'(n_h x) - n_h \psi_n(n_h x)\psi_n'(n_s x)}{n_s \psi_n(n_s x)\xi_n'(n_h x) - n_h \xi_n(n_h x)\psi_n'(n_s x)}, \tag{3}$$

$$b_n^{\text{Mie}} = \frac{n_h \psi_n(n_s x)\psi_n'(n_h x) - n_s \psi_n(n_h x)\psi_n'(n_s x)}{n_h \psi_n(n_s x)\xi_n'(n_h x) - n_s \xi_n(n_h x)\psi_n'(n_s x)}. \tag{4}$$

Here $x = \omega r_s / c$, the functions $\psi_n(z)$ and $\xi_n(z)$ are Riccati-Bessel functions,[12] and primes indicate differentiation with respect to the argument.

Usually, when the constituent particles are nonmagnetic,

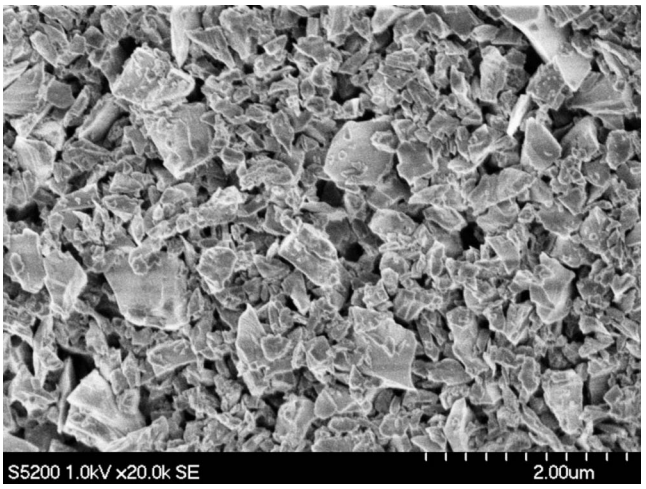

FIG. 1. SEM image of the SiC powder sample.

there is no induced magnetic-dipole response b_1 in the long-wavelength limit and $\mu_{\text{eff}}=\mu_0$. However, this is no longer true if the particles have a large permittivity,[8] such that $|\varepsilon_s|/\varepsilon_h$ is roughly 100. Then each particle acts as a resonator with circulating displacement currents, which is a magnetic-dipole mode. Some dielectrics have infrared phonon-polariton resonances that are strong enough to satisfy this condition, and for our study we use particles of α (hexagonal) SiC, whose permittivity function is

$$\varepsilon_s(\omega) = \varepsilon_\infty\left(1 + \frac{\omega_L^2 - \omega_T^2}{\omega_T^2 - \omega^2 - i\omega\gamma}\right), \tag{5}$$

where $\varepsilon_\infty=6.7$ is the high-frequency limit of the permittivity, $\omega_T=790$ cm^{-1} is the transverse optical phonon frequency, $\omega_L=966$ cm^{-1} is the longitudinal optical phonon frequency, and $\gamma=5$ cm^{-1} is the damping coefficient.[13] The permittivity ε_s is extremely large at frequencies near and below ω_T, and the real part is negative for $\omega_T<\omega<\omega_L$. Furthermore, for experimental reasons it is necessary to dilute the sample with a host material of KBr ($n_h=1.5$). For spherical SiC particles, the electric-dipole resonances are roughly size independent, occurring when $\varepsilon_s=-2\varepsilon_h$. However, the magnetic-dipole resonant frequency ω_m is size dependent,[8] resonating when the permittivity is large at frequencies slightly below ω_T, when $\omega_m \approx \pi c/(|n_s|r_s)$.

Our sample is a powder of α-SiC purchased from Alfa-Aesar, USA (item no. 40155). A scanning electron microscopy (SEM) image is shown in Fig. 1. The sample was fabricated by mechanical milling and as such the size distribution can be modeled with a normalized log-normal[14] number density distribution

$$\frac{d\phi}{dr} = \frac{1}{r}\frac{d\phi}{d\ln r} = \frac{1}{r\ln\sigma_g\sqrt{2\pi}}\exp\left[\frac{-(\ln r - \ln r_g)^2}{2\ln^2\sigma_g}\right]. \tag{6}$$

Thus the size average of any quantity $f(r)$ is $\langle f(r)\rangle = \int_0^\infty f(r)\frac{d\phi}{dr}dr$. For our sample the median size is $2r_g = 0.7$ μm, the geometric standard deviation is $2\sigma_g=1.5$, and the maximum particle size is roughly 2 μm. These particles are small enough that both the effective-medium approximation is valid and higher multipole scattering is negligible. All sizes of these particles support electric-dipole resonances, while *only particles larger than roughly* 0.5 μm support magnetic-dipole resonances.

The sample of irregularly shaped particles cannot be modeled as spheres using Mie theory. To determine how to model them we first consider the scattering properties of spheroidal particles, whose shapes are a subset of ellipsoids in which the lengths of two of the three principle axes are equal. The shape of a spheroid is described by a vertical to rotational axis ratio a/b (see inset of Fig. 2), such that oblate (cigar-shaped) spheroids have $a/b<1$ and prolate (pancake-shaped) spheroids have $a/b>1$. We calculate numerically, using a T-MATRIX code,[15] the orientation-averaged volume-normalized extinction cross sections C_{ext}/V for various shapes of spheroids as shown in Fig. 2. Each particle size is such that its longest axial length is 0.7 μm (which is the median size in our sample).

All cases in Fig. 2 have a magnetic-dipole resonance near 785 cm^{-1}, indicating its weak dependence on the particle shape. This is because the resonant magnetic-dipole field is contained within the volume of the particle. Furthermore, any frequency shift caused by the size distribution is compensated by the rapid increase of $|n_s|$ for this frequency range just below ω_T, which is due to the phonon-polaritonic SiC. The magnetic response can therefore be approximated by the magnetic-dipole Mie coefficient even though the particles are not spheres. Hence, the shape and orientation averaging are trivial: $\overline{b_1} \approx b_1^{\text{Mie}}$. The extinction C_{ext}, scattering C_{sca}, and absorption C_{abs} cross sections are the quantities required for

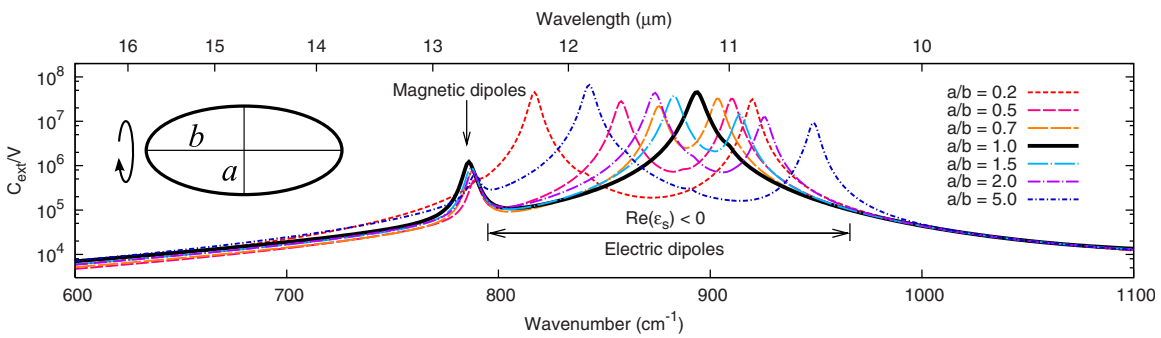

FIG. 2. (Color online) Volume-normalized extinction cross sections of various shapes of spheroidal SiC particles. Each curve represents a single particle in a KBr host, averaged over all orientations.

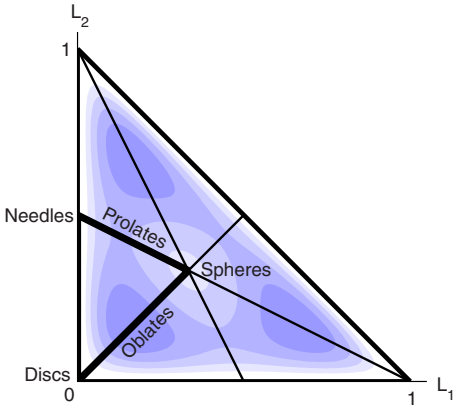

FIG. 3. (Color online) The shape probability density function $p(L_1,L_2)$ used to model the SiC powder. The outer triangle is the domain of geometric factor pairs (L_1,L_2). Points within one subtriangle describe unique ellipsoidal shapes, while the remaining subtriangles represent other orientations.

modeling our experimental results, and the magnetic-dipole contributions to them are

$$\langle \overline{C_{\text{ext,mag}}} \rangle \approx \frac{6\pi}{k_h^2} \langle \text{Re}\{b_1^{\text{Mie}}\} \rangle, \tag{7a}$$

$$\langle \overline{C_{\text{sca,mag}}} \rangle \approx \frac{6\pi}{k_h^2} \langle |b_1^{\text{Mie}}|^2 \rangle, \tag{7b}$$

$$\langle \overline{C_{\text{abs,mag}}} \rangle = \langle \overline{C_{\text{ext,mag}}} \rangle - \langle \overline{C_{\text{sca,mag}}} \rangle, \tag{7c}$$

which are the same as from Mie theory.[11]

In contrast to the magnetic-dipole resonance, the deformation of a sphere splits the electric-dipole resonance from 895 cm^{-1} (the solid curve in Fig. 2) to other frequencies within the range where $\text{Re}\{\varepsilon_s\}<0$. This dramatic effect must be captured in the theory, so the Mie coefficient a_1^{Mie} is unsuitable as the generalized electric-dipole coefficient. Instead, we generalize the particle shapes further to ellipsoids. An ellipsoid generally has three unequal semiaxis lengths a, b, and c, and its shape depends on only two ratios of these lengths. However, it is more convenient to classify the particle shapes in terms of geometrical factors L_j, $j=1,\ldots,3$, which are related to the semiaxes through an elliptical integral[11] and satisfy $0\leq L_j \leq 1$ with $L_1+L_2+L_3=1$. Since only two of the geometrical factors are independent, the domain of values (L_1,L_2) can be plotted as shown in the largest triangle in Fig. 3. Only one of the six subtriangles describes all possible unique shapes, while the remaining subtriangles describe other orientations. The notable shapes of spheres, infinitely thin disks, and needles are indicated in the figure, and points on the interior lines describe spheroids. Using an electrostatic approximation,[11] the electric polarizability along the principle axis j is

$$\alpha_{e,j} \approx \frac{V}{\beta + L_j}, \tag{8}$$

where V is the particle volume and $\beta=\varepsilon_h/(\varepsilon_s-\varepsilon_h)$.

Furthermore, a normalized shape distribution of ellipsoids $p(L_1,L_2)$ must be included. The simplest choice is a uniform distribution,[11] where $p(L_1,L_2)=2$. Although this distribution is convenient, it overestimates the presence of extremely eccentric particles. Ossenkopf *et al.*[16] proposed a more realistic distribution, $p(L_1,L_2)=120L_1L_2L_3$, which eliminates the probability of infinitely eccentric particles in which at least one $L_j=0$. We refine this distribution to account for the relative lack of spheres in our sample in Fig. 1

$$p(L_1,L_2) \propto L_1L_2L_3\left[\sum_{j=1}^{3}\left(L_j-\frac{1}{3}\right)^2 + C\right], \tag{9}$$

where we set $C=0.05$. The level contours of this function are shown in Fig. 3, where it is seen that this distribution favors moderately eccentric ellipsoids. We can now determine the electric-dipole contributions to the various cross sections

$$\langle \overline{C_{\text{ext,elec}}} \rangle = \langle \overline{C_{\text{sca,elec}}} \rangle + \langle \overline{C_{\text{abs,elec}}} \rangle, \tag{10a}$$

$$\langle \overline{C_{\text{sca,elec}}} \rangle \approx \frac{k_h^4}{6\pi}\sum_{j=1}^{3}\frac{1}{3}\langle \overline{|\alpha_{e,j}|^2} \rangle = \frac{k_h^4}{6\pi}\langle V^2 \rangle \int\int_{\Delta} dL_1 dL_2 \left|\frac{p(L_1,L_2)}{\beta+L_1}\right|^2, \tag{10b}$$

$$\langle \overline{C_{\text{abs,elec}}} \rangle \approx k_h \,\text{Im}\sum_{j=1}^{3}\frac{1}{3}\langle \overline{\alpha_{e,j}} \rangle = k_h \langle V \rangle \text{Im}\left\{\int\int_{\Delta} dL_1 dL_2 \frac{p(L_1,L_2)}{\beta+L_1}\right\}, \tag{10c}$$

where the domain Δ of the double integrals is the large triangle shown in Fig. 3. These integrals take into account all shapes and orientations and can be evaluated in closed form using the distribution in Eq. (9). Note that due to the electrostatic approximation of Eq. (8), the extinction cross section must be calculated by the optical theorem.[11] Although the volume V of a particle depends on its shape and therefore $V(L_1,L_2)$, for simplicity we assume the volume of a sphere only. This same simplification is also implicit in the magnetic-dipole terms of Eq. (7), since $b_1^{\text{Mie}} \propto V$, and the error introduced by this simplification is not of much consequence. The overall cross sections are then the sums of the magnetic (7) and electric (10) contributions. Furthermore, the average generalized electric-dipole coefficient used in Eq. (2) is then $\langle \overline{a_1} \rangle = k_h^3 \langle \overline{\alpha_{e,1}} \rangle / 6\pi i$.

The response of the SiC powder sample was measured using diffuse reflectance techniques.[17] A sample was prepared by mixing a small amount of the SiC powder with powdered KBr and placed in a metal sample cup to a depth of 5 mm. A Fourier transform infrared (FTIR) spectrometer (Perkin-Elmer Spectrum BX) was used with a deuterated triglycine sulfate (DTGS) detector. The incident and reflected beams were condensed with ellipsoidal mirrors, which provide diffuse incidence and collection. The diffuse radiation penetrating the sample surface can be multiply reflected, scattered, or absorbed by the SiC within the sample mixture. The measured diffuse reflectance spectrum is shown in Fig. 4.

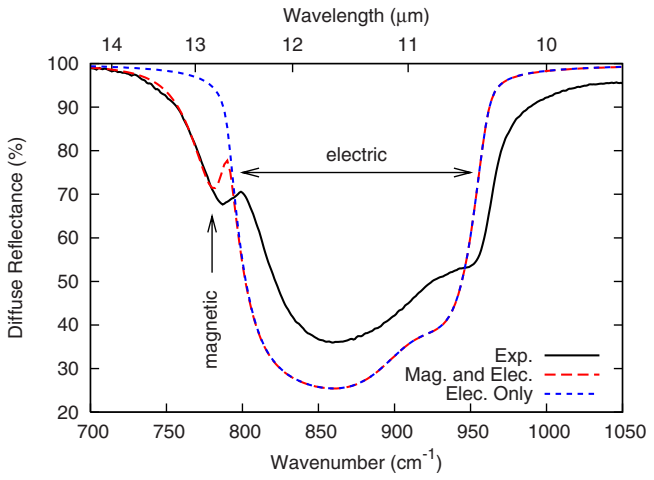

FIG. 4. (Color online) The diffuse reflectance of a dilute mixture of the SiC powder sample in a KBr host.

The diffuse reflectance R can be calculated with the general Kubelka-Munk equation[18]

$$R = \frac{1 - R_b[A - B\coth(BSh)]}{A + B\coth(BSh) - R_b}, \tag{11}$$

where R_b is the reflectance of the metal sample cup, $A=(S+K)/S$, $B=\sqrt{A^2-1}$, $h=5$ mm is the thickness of the sample mixture, K is an absorption coefficient, and S is a scattering coefficient. Although K and S are phenomenological values, it has been shown[19] that they are roughly $K \approx 2N\langle C_{\mathrm{abs}}\rangle$ and $S \approx N\langle C_{\mathrm{sca}}\rangle$, where these cross sections are the sums of appropriate terms in Eqs. (7) and (10). Two cases of calculated diffuse reflectance are shown in Fig. 4, where we use $R_b=1$ to model the metal sample cup, and $N=5\times10^{13}$ m^{-3}. One of the cases includes both the magnetic and electric-dipole contributions from Eqs. (7) and (10), while the other includes only the quasistatic electric-dipole contributions (10). This demonstrates that the broad peak from 800 to 960 cm^{-1} is the electric-dipole resonance, while the peak around 785 cm^{-1} is the magnetic-dipole response of the dielectric particles. The theory agrees well with the measurement, except for a small overall shift in frequency, and for slightly unequal magnetic-to-electric resonant strength ratio, which is quite likely due to the approximate statistics used to generalize the theory to random particles. Nevertheless, our model captures all of the essential features of the crude and random mixture. The constant C of Eq. (9) only affects the match of the shoulder in the electric resonance from 870 to 930 cm^{-1}. Due to the sensitivity of the diffuse reflectance technique, the particle density N must be quite small, so the effective permeability and permittivity corresponding to these results are both positive. However, with improved particle filtering and experimental techniques, a true negative permeability metamaterial may be produced.

To conclude, we have developed a model of the scattering and effective-medium properties of randomly shaped SiC microparticles. The model approximates the magnetic-dipole scattering as though the particles were spheres using Mie theory, and uses an ellipsoidal electrostatic approximation for the electric-dipole scattering. Furthermore, size, shape, and orientation distributions are included in our model. The diffuse reflectance, calculated with the general Kubelka-Munk equation, matches experimental infrared spectroscopic measurements well and indicates both infrared magnetic and electric-dipole responses in a purely dielectric sample. This demonstrates that magnetic metamaterials need not require sophisticated fabrication techniques and should greatly simplify their implementation and application, especially as an element in negative index metamaterials.

*mark.wheeler@utoronto.ca

[1] J. B. Pendry, Phys. Rev. Lett. **85**, 3966 (2000).
[2] D. Schurig, J. J. Mock, B. J. Justice, S. A. Cummer, J. B. Pendry, A. F. Starr, and D. R. Smith, Science **314**, 977 (2006).
[3] V. M. Shalaev, Nat. Photonics **1**, 41 (2007).
[4] N. Liu, H. Guo, L. Fu, S. Kaiser, H. Schweizer, and H. Giessen, Nature Mater. **7**, 31 (2008).
[5] C. L. Holloway, E. F. Kuester, J. Baker-Jarvis, and P. Kabos, IEEE Trans. Antennas Propag. **51**, 2596 (2003).
[6] M. S. Wheeler, J. S. Aitchison, and M. Mojahedi, Phys. Rev. B **72**, 193103 (2005).
[7] V. Yannopapas and A. Moroz, J. Phys.: Condens. Matter **17**, 3717 (2005).
[8] M. S. Wheeler, J. S. Aitchison, and M. Mojahedi, Phys. Rev. B **73**, 045105 (2006).
[9] J. A. Schuller, R. Zia, T. Taubner, and M. L. Brongersma, Phys. Rev. Lett. **99**, 107401 (2007).
[10] Q. Zhao, L. Kang, B. Du, H. Zhao, Q. Xie, X. Huang, B. Li, J. Zhou, and L. Li, Phys. Rev. Lett. **101**, 027402 (2008).
[11] C. F. Bohren and D. R. Huffman, *Absorption and Scattering of Light by Small Particles* (Wiley, New York, 1983).
[12] *Handbook of Mathematical Functions with Formulas, Graphs, and Mathematical Tables*, edited by M. Abramowitz and I. A. Stegun (Dover, New York, 1972).
[13] W. G. Spitzer, D. Kleinman, and D. Walsh, Phys. Rev. **113**, 127 (1959).
[14] T. Allen, *Particle Size Measurement*, 5th ed. (Kluwer, Dordrecht, 1999), Vol. 1.
[15] M. I. Mishchenko and L. D. Travis, J. Quant. Spectrosc. Radiat. Transf. **60**, 309 (1998).
[16] V. Ossenkopf, T. Henning, and J. S. Mathis, Astron. Astrophys. **261**, 567 (1992).
[17] M. P. Fuller and P. R. Griffiths, Anal. Chem. **50**, 1906 (1978).
[18] P. Kubelka, J. Opt. Soc. Am. **38**, 448 (1948).
[19] A. Ishimaru, *Wave Propagation and Scattering in Random Media* (IEEE, New York, 1997).